



Contents lists available at ScienceDirect

## Earth and Planetary Science Letters

www.elsevier.com/locate/epsl



## Tectonic tremor and slow slip along the northwestern section of the Mexico subduction zone

Michael R. Brudzinski<sup>a</sup>, Kristen M. Schlanser<sup>a,1</sup>, Nicholas J. Kelly<sup>a,2</sup>, Charles DeMets<sup>c</sup>, Stephen P. Grand<sup>b</sup>, Bertha Márquez-Azúa<sup>d</sup>, Enrique Cabral-Cano<sup>e</sup>

<sup>a</sup> Miami University of Ohio, United States

<sup>b</sup> University of Texas, United States

<sup>c</sup> University of Wisconsin–Madison, United States

<sup>d</sup> Universidad de Guadalajara, Mexico

<sup>e</sup> Universidad Nacional Autónoma de México, Mexico

### ARTICLE INFO

#### Article history:

Received 30 March 2016

Received in revised form 1 August 2016

Accepted 2 August 2016

Available online xxxxx

Editor: P. Shearer

#### Keywords:

tremor  
subduction  
Mexico  
slow slip  
earthquake  
GPS

### ABSTRACT

The southwestern coast of Mexico is marked by active subduction of the Rivera and Cocos plates, producing megathrust earthquakes that tend to recur every 50–100 yr. Herein, we use seismic and GPS data from this region to investigate the potential relationship between earthquakes, tectonic (non-volcanic) tremor, and transient slip along the westernmost 200 km of the Mexico subduction zone. Visual examination of seismograms and spectrograms throughout the 18-month-long MARS seismic experiment reveals clear evidence for frequent small episodes of tremor along the Rivera and Cocos subduction zones beneath the states of Jalisco, Colima, and Michoacán. Using a semi-automated process that identifies prominent energy bursts in envelope waveforms of this new data, analyst-refined relative arrival times are inverted for source locations using a 1-D velocity model. The resulting northwest–southeast trending linear band of tremor is located downdip from the rupture zones of the 1995 Mw 8.0 Colima–Jalisco and 2003 Mw 7.2 Tecoman subduction-thrust earthquakes and just below the regions of afterslip triggered by these earthquakes. Despite the close proximity between tremor and megathrust events, there is no evidence that the time since the last great earthquake influences the spatial or temporal pattern of tremor. A well-defined gap in the tremor beneath the western Colima Graben appears to mark a separation along the subducted Rivera–Cocos plate boundary. From the position time series of 19 continuous GPS sites in western Mexico, we present the first evidence that slow slip events occur on the Rivera plate subduction interface. Unlike the widely-recorded, large-amplitude, slow slip events on the nearly horizontal Cocos plate subduction interface below southern Mexico, slow slip events below western Mexico have small amplitudes and are recorded at relatively few, mostly coastal stations. The smaller slow slip beneath western Mexico may be due to the steeper dip, causing a narrower zone where the conditions for slow slip are met. The prominent afterslip following the M = 8 1995 Colima–Jalisco and M = 7.2 2003 Tacoma megathrust earthquakes may also shrink the area available for episodic slow slip.

© 2016 Elsevier B.V. All rights reserved.

## 1. Introduction

The theoretical downdip limit of a plate interface seismogenic zone is marked by a transition from stick-slip to stable sliding behavior (Scholz, 2002). Recent advances in seismic and geodetic monitoring have led to improved measurements of fault structure

and behavior where this transition is expected, including the discovery of a family of slow fault slip phenomena (Schwartz and Rokosky, 2007). Careful analysis of the positions of GPS instruments near the edge of the plate relative to those in the interior found that some instruments were repetitively moving back toward the trench, similar to earthquakes but much more gradually over the span of several weeks and in some cases over a year (Rogers and Dragert, 2003). Curiously, the largest transient motions were not recorded at the coast above the locked zone but farther inland, indicating slow slip occurs deeper on the plate interface. While episodic slow slip differs from earthquakes in many

E-mail address: brudzimr@miamioh.edu (M.R. Brudzinski).

<sup>1</sup> Now at University of Cincinnati.

<sup>2</sup> Now at Ohio State University.

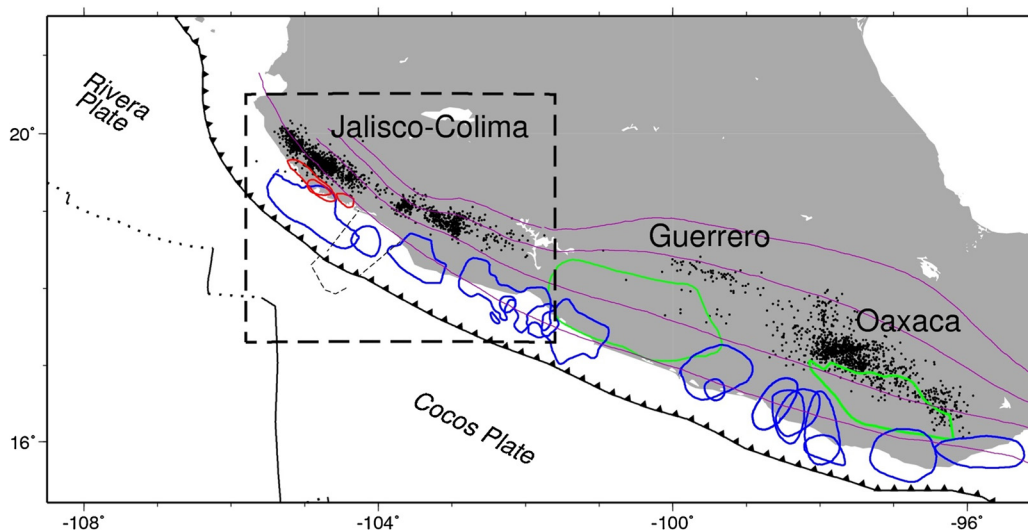


**Fig. 1.** Map of southern Mexico showing observed source regions of megathrust earthquakes (blue), afterslip (red), episodic transient slip (green), and tectonic tremor (black). Dashed box marks the focus of this study in the states of Jalisco, Colima and Michoacán (Fig. 2). Previous results for tremor and slip are from the states of Guerrero and Oaxaca (Payero et al., 2008; Brudzinski et al., 2010; Radiguet et al., 2012; Fasola et al., 2016). Thin dashed line marks the Manzanillo Trough and purple lines show slab contours (Pardo and Suárez, 1995). (For interpretation of the references to color in this figure legend, the reader is referred to the web version of this article.)

ways, it can still be accompanied by low-level seismic vibrations referred to as non-volcanic tremor (Rogers and Dragert, 2003). The term tremor was applied to these weak signals as they are emergent, meaning they gradually appear out of the background noise, and often undulate with slowly varying amplitudes (Obara, 2002). However, they differ from typical volcanic tremor both in their deep source region and in the lack of harmonic peaks in their frequency content (Schwartz and Rokosky, 2007). This type of tremor has a narrow frequency band of 1–10 Hz and appears to be composed of a swarm of low-frequency earthquakes (Shelly et al., 2007), as traditional earthquakes of similar size would have more energy at higher frequencies (Kao et al., 2009). Nevertheless, estimates of the focal mechanism suggest this tremor and low-frequency earthquakes are produced by shear faulting (Ito et al., 2007), and detailed location techniques find the sources align with the plate interface (Brown et al., 2009), so tectonic tremor seems to be an appropriate term.

The first reports of slow slip and tremor in Mexico came from the Guerrero region (Fig. 1), with remarkably large ( $M_w \sim 7.5$ ) episodic transient slip (Kostoglodov et al., 2003; Radiguet et al., 2012) and tectonic tremor that appeared to be most prominent during slow slip (Payero et al., 2008; Frank et al., 2015) (Fig. 1). Southeast in Oaxaca (Fig. 1), GPS measurements reveal transient slip episodes every 12 to 24 months that can last several months (Brudzinski et al., 2007; Graham et al., 2015). Episodes of tremor in Oaxaca last upwards of a week and recur as frequently as every 2–3 months in a given region, but do not coincide in time or space with transient slip events (Brudzinski et al., 2010). Epicenters of tremor bursts primarily occur between the 25–50 km contours for depth of the plate interface (Fig. 1) (Fasola et al., 2016). In central Oaxaca, tremor hypocenters correlate well with a high conductivity zone that is interpreted to be due to slab fluids (Jödicke et al., 2006). In both Oaxaca and Guerrero, tremor is primarily located further inland than GPS-detected slow slip (Fig. 1), while the latter is associated with a zone of ultra-slow velocity interpreted to represent high pore fluid pressure (Song et al., 2009). This zone of slow slip corresponds to approximately 350–450 °C (Currie et al., 2002), with megathrust earthquakes, microseismicity, and strong long-term coupling occurring immediately updip from it. This leaves tremor primarily in a region further inland from the thermally defined transition zone, suggesting that

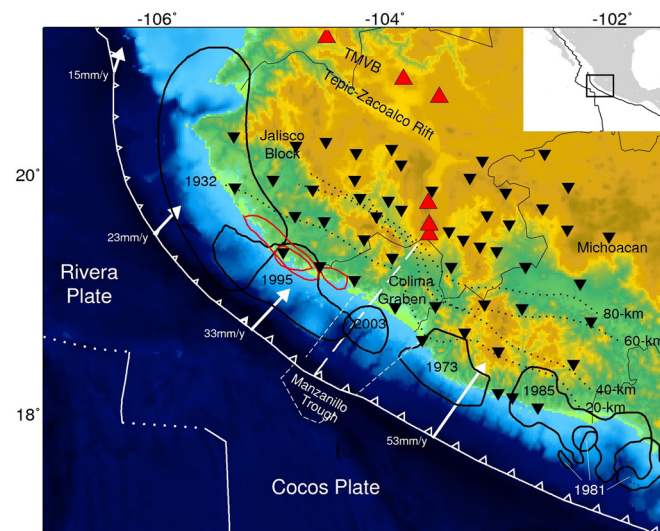


**Fig. 2.** Map of southwestern Mexico showing the focus area of this study. Seismic stations of the MARS temporary deployment are inverted triangles. Thick solid lines encircle approximate megathrust rupture zones (numbers indicate year) (Reyes et al., 1979; Mendoza, 1993; Schmitt et al., 2007) and red lines encircle areas of prominent afterslip following the 1995 earthquake (Hutton et al., 2001). Thin solid lines show state borders. Dotted lines show slab contours established with the MARS network (Abbott and Brudzinski, 2015). Dashed lines mark the Manzanillo Trough and red triangles show volcanoes. (For interpretation of the references to color in this figure legend, the reader is referred to the web version of this article.)

transition from locking to free slip may occur in more than one phase.

In this study, we focus our attention on the western end of the Mexican subduction zone, where deployments of geodetic and seismic instruments provide new opportunities to investigate tremor and transient slip in a region where several large megathrust earthquakes have occurred during modern instrumental recording (Fig. 2) (Abbott and Brudzinski, 2015 and references therein). The first was the 1973 January 30 ( $M_w$  7.6) Colima earthquake that occurred just to the southeast of the Manzanillo Trough and Colima Graben, which are sediment filled structures that appear to accommodate trench-parallel extension (e.g., Bandy et al., 1995). The 1995 October 9 ( $M_w$  8.0) Colima–Jalisco earth-

quake (Fig. 2) was one of the first earthquakes to have occurred close enough to a GPS geodetic network to study the coseismic and near-term post-seismic behavior of the subduction fault interface. This earthquake was the first significant rupture northwest of the Manzanillo Trough since the 1932 June 3 (Mw ~8.2) and 1932 June 18 (Mw ~7.8) earthquakes (Singh et al., 1985). While the extent of these earlier ruptures is not well known, the former is thought to include the 1995 rupture zone and a portion of the interface further to the north. The geodetic and seismologic results concur that slip was largely focused above depths of 20 km along a ~150 km segment extending northwest from the edge of the Manzanillo Trough (Mendoza and Hartzell, 1999; Hutton et al., 2001). The most recent large megathrust earthquake to occur in our study region was the 2003 January 22 (Mw 7.2) Tecomán earthquake offshore from Colima (Fig. 2). Seismic and geodetic inversions indicate that most and possibly all of the coseismic slip was limited to a 80 km along-strike region that is bounded by the Manzanillo Trough (Schmitt et al., 2007). The apparent coincidence of the edges of the 1932, 1973, 1995 and 2003 rupture sequences with the edges of the Manzanillo Trough indicate that it may represent a mechanical barrier to along-strike rupture propagation.

The Manzanillo Trough and Colima Graben mark a region of particular tectonic interest, because both are near the intersection of the subducting Rivera and Cocos plates (Singh et al., 1985; Bandy et al., 1995) and mark the eastern extent of the elevated Jalisco Block (Fig. 2). This region is one of the few places on Earth where young (<11 Myr), subducting oceanic lithosphere undergoes microplate fragmentation and capture (Fig. 2). The Rivera plate appears to have separated from the Cocos plate 5–10 Ma, but the boundary and relative motion between the plates are still debated (e.g., DeMets and Wilson, 1997; Bandy et al., 1998). Subduction of the Rivera plate is nearly perpendicular to the trench beneath Colima at a rate of ~40 mm/yr, but becomes progressively more oblique and slower to the northwest (DeMets and Wilson, 1997). To the southeast, the Cocos plate subducts at ~50 mm/yr, implying that motion occurs between the subducting Rivera and Cocos slabs beneath the continental margin. Although a great deal of geodetic, petrologic, structural, and paleomagnetic work has been done in the region there has been no detailed study of the deeper part of the plate interface. Thus, little is known about how subduction of young lithosphere that is actively experiencing microplate fragmentation influences deformation between the subducting and overriding plates.

The MARS (Mapping the Rivera Subduction Zone) experiment consisted of the deployment of 50 temporary broadband seismic instruments in a two dimensional array deployed in southwestern Mexico for 18 months from January 2006 to June 2007 (Fig. 2). While characterizing tectonic tremor was not an original target of this experiment (e.g., Yang et al., 2009), the deployment configuration is ideally situated to examine a ~400-km along-strike section of the transition zone of the plate interface, where tremor has been observed in several other subduction zones. In this study, we first seek to establish the existence and prevalence of tectonic tremor across the Jalisco, Colima, and western Michoacán states. We analyze waveforms for tremor source locations, which we use to investigate the behavior of the plate interface across the subducted boundary between the Rivera and Cocos plates. We utilize continuous GPS time series to ascertain whether a relationship exists between tremor and transient slip. Considering that the time since the last megathrust earthquake varies along strike in this region, we also compare the patterns in tremor activity to test hypotheses about the behavior of tremor at different points in the earthquake cycle.

## 2. Evidence for tectonic tremor and its temporal variation

Our search for tremor begins with visual inspection of bandpass (2–5 Hz) filtered hour-long envelope seismograms from the quietest stations in the network to see whether there were coherent changes in amplitude across the network. To reduce the influence of cultural noise that produces considerable fluctuations over the course of the day at some stations, we restrict our scan to nighttime hours. We find many cases where the amplitudes wax and wane coherently at neighboring stations for several days (Fig. 3). The emergent nature and long durations of the apparent tremor signals clearly distinguish them from earthquakes (Obara, 2002), where earthquakes appear as abrupt increases with a rapid decay in hour-long envelope seismograms. The coherent changes in amplitude between neighboring stations over minute-to-hour time scales indicate they are not due to cultural noise local to a given site which would be variable from station to station on those time scales. The fact that not all network sites show the raised amplitudes during a given episode and that they appear strongest on inland stations further indicates they are more likely due to tremor than weather or ocean-related noise. The latter issue is also addressed by confirming that tropical storms are not responsible for any of the apparent tremor episodes documented in this study (<http://www.solar.ifa.hawaii.edu/Tropical/Data/>). Instead, Fig. 3 shows 6 examples of days with increased activity in the tremor passband throughout the 18 months of recording, when the amplitudes tend to be raised at either eastern, central, or western stations, suggesting these signals originate in various regions within our network.

We next examine bursts of energy within the time periods of raised amplitudes to see whether they are consistent with a coherent non-earthquake source. These bursts of energy have typical durations of 10 s, and the filtered envelope seismograms show relative arrival times between stations with an expected moveout pattern for events within our network (Fig. 4). These moveouts are the primary information used to investigate source locations in the next section. We also produce spectrograms for the bursts of energy to confirm that the signals are primarily restricted to the 1–10 Hz passband expected for tectonic tremor (Obara, 2002), whereas local earthquakes typically have prominent energy above 10 Hz (Fig. 4). This last comparison is important because microseismicity is common in this region, so it is checked on a regular basis to confirm the authenticity of tremor signals.

With several pieces of evidence that tectonic tremor exists in this region, we next determine the temporal fluctuations of this tremor. Our initial attempt to characterize this was to utilize the mean amplitude scanning technique (Brudzinski and Allen, 2007; Brudzinski et al., 2010). Application of this technique produces mixed results in this region (Fig. 5). There are a number of peaks that rise above the background at several stations, such that initial processing for tremor source locations is focused during these times. However, there are a large number of smaller peaks throughout the mean amplitude time series which have variable levels of correlation at neighboring stations that make it unclear whether these peaks are due to tremor or cultural noise. In hindsight, most of these peaks are in fact associated with tremor, but the episode durations, recurrence, and spatial extent are small, which leads to many small peaks that do not correlate well across several stations.

To more thoroughly investigate when tremor is occurring across our network, we utilize visual inspection of bandpass filtered hour-long envelope seismograms from the quietest stations in the network. This follows the approach first applied in Nankai where the original tremor and LFE catalogs were made through visual identification by analysts at JMA and NEID (e.g., Obara, 2002; Shelly et al., 2007). Our approach involves three analysts inde-

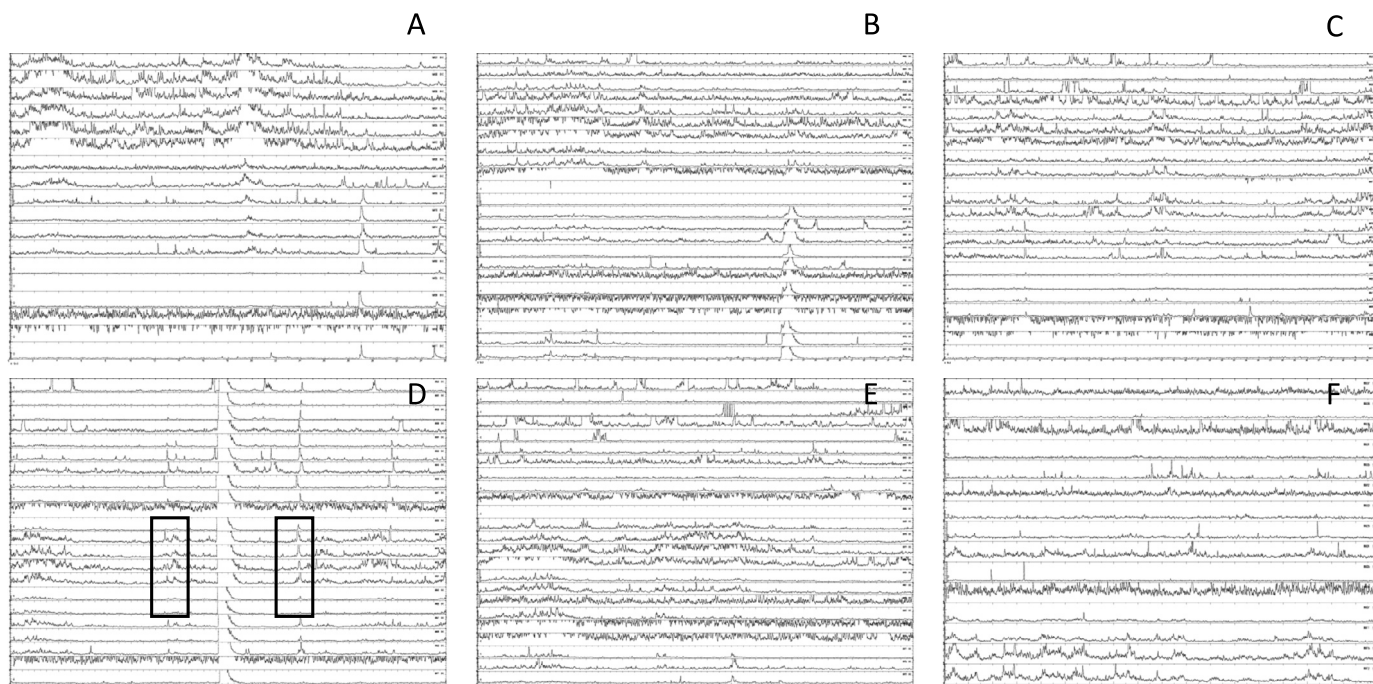


**Fig. 3.** Hour-long envelope seismograms illustrating subtle correlated, undulating signals at several neighboring stations which are evidence for tectonic tremor. Seismograms are filtered (2–5 Hz) horizontal component with the instrument response removed. All are plotted at the same amplitude scale, sorted from west to east. Only stations from the MARS deployment with relatively low noise levels and at least one instance of a tremor signal correlated with other stations are shown. Number of stations shown varies due to different station record times (Fig. 6). This view of hour-long seismograms was used to visually scan for tremor signals over the entire MARS deployment. These six time periods are shown to illustrate representative signals from different source regions moving from west (A) to east (F). For comparison, prominent earthquake signals can be found in the western part of (B) and all across (D). Boxes in (D) show sections of seismograms analyzed in Fig. 4.

pendently examining plots of nighttime hours during the entire 18 months of data, marking whether strong or weak tremor is occurring in the eastern, central, and/or western part of the network. Fig. 6 shows the combined results of this scan. Strong episodes of tremor are most prevalent in the western end of the network, but still common in the central and eastern ends of the network. Characterizing the eastern end of the network is essentially limited to  $\sim 7$  months when there are sufficient stations to identify and locate tremor in that region.

### 3. Spatial distribution of tectonic tremor

Previous analyses of source locations of tectonic tremor in the Cascadia and Oaxaca regions have been conducted using a semi-automated algorithm for finding individual bursts during hours with large mean amplitudes in the tremor passband, and have used relative arrival times across seismic networks to determine the source locations (Boyarko and Brudzinski, 2010; Brudzinski et al., 2010). This process begins the same way as the mean amplitude scanning algorithm that removes the instrument response from an hour-long seismogram, bandpass filters at 1–6 Hz, takes the absolute value and calculates envelope seismograms. Considering the similarity in processing, it was natural to focus our attention on hours with large mean amplitudes. To help clarify the bursts of energy in a given hour from station to station, we smooth the envelopes with a 0.06 s low-pass filter and stack the three components to enhance tremor signals with respect to background noise.

To identify when signals are most active across our network, we examine a record section of all the station time series together. We target distinct prominent pulses rising above background noise in this seismic network activity time series. For each peak time, we examine envelope waveforms around that time for stations that have signal to noise ratios of at least 1.5. For cases with coherent signals and reasonable moveouts, we select the peak times

that best represent the station-to-station relative timing of energy packets and treat them as S wave arrival times. This approach is dictated by the emergent nature of tremor and small signal to noise ratios, but we estimate that the median picking uncertainty is less than 1 s based on evaluation of over 100 waveforms.

When a coherent tremor burst is observed at a minimum of five stations, the analyst-refined arrival times are used to invert for a source location using a 1D approximation of the regional S wave velocity model that was previously constructed based on gravity data, seismicity, and attenuation (Cruz-Jiménez et al., 2009). The source inversion is performed using the computationally efficient ELOCATE algorithm (Hermann, 2004), which also produces nominal uncertainties based on incoherence between arrival times. We also recalculated locations many times by randomly adjusting arrival times between  $-1.0$  and  $1.0$  s to estimate the location uncertainty potentially due to picking error. In addition, we obtained formal location uncertainty estimates based on bootstrap location reliability (Wech and Creager, 2008). For each event we iteratively remove each station from the input arrival times, one at a time, and search for a location. We interpret the median of the resulting cloud of locations as the source centroid epicenter with an error estimated by the median absolute deviation. This processing and the resulting uncertainties are similar to comparable analysis of tremor in Oaxaca (Brudzinski et al., 2010).

Fig. 7 shows the distribution of tremor sources we have identified in this study. Within the overall tremor band, the number of sources we can locate is not homogeneous along-strike (Fig. 7b). We find four clusters of events, which do not reflect individual episodes as they are active in several episodes. Two western clusters are separated from two eastern clusters, with a definitive gap in the center that is not due to lack of station coverage or quality. The far eastern region also produced some tremor locations (Fig. 7a), but there are fewer stations and more gaps in record-

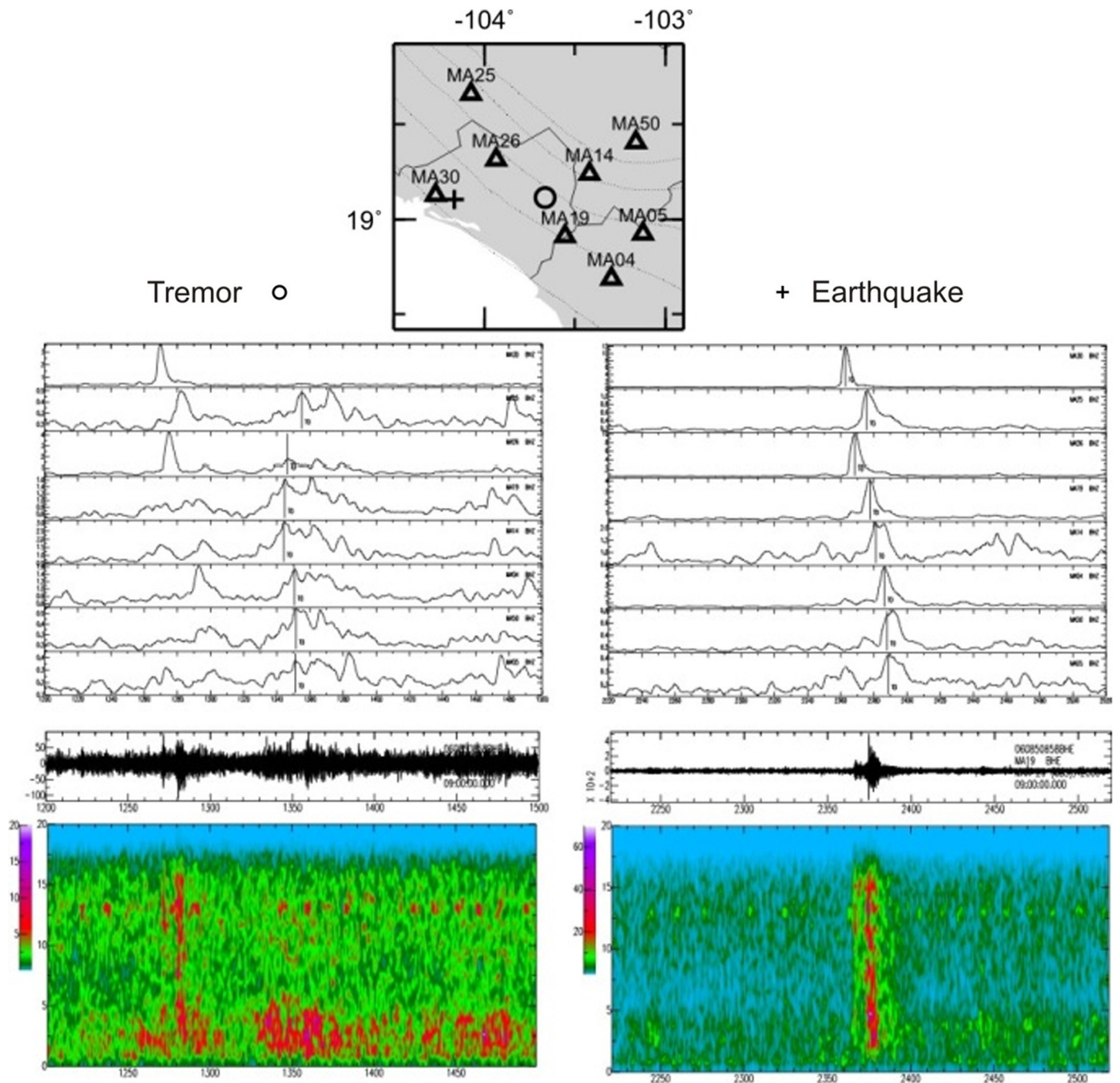


**Fig. 4.** Comparison of representative tectonic tremor and local earthquake signals from March 26, 2006. (Top panel) Map of stations and epicenters for an example tremor burst (circle) and earthquake (cross). (Middle panel) Smoothed envelope waveforms for stations from west to east, with phase pick marked by the vertical line. (Bottom panel) A 1–20 Hz filtered seismogram from a station near the epicenter and its corresponding spectrogram. (For interpretation of the colors in this figure, the reader is referred to the web version of this article.)

ing in the region which makes it difficult to obtain locations at this end of the network. We note that tremor in the western clusters are closer to the coastline than in the eastern clusters. This does not appear to be a result of slab dip, because a recent study of slab geometry using the MARS deployment found that Rivera plate subduction interface has a shallower dip in the west than that of the Cocos plate in the east (Abbott and Brudzinski, 2015). The depth resolution of tremor hypocenters using the semi-automated approach is poor (e.g., Brudzinski et al., 2010), but studies indicate tremor occurs on or very near the plate interface (e.g., Brown et al., 2009), so the slab depth contours of Abbott and Brudzinski (2015) provide a useful guide. The slab

depth contours suggests that tremor associated with the Rivera plate occurs at 15–40 km depth. Tremor associated with the Cocos plate in the easternmost cluster occurs at 35–75 km, but appears to shift shallower in the cluster closer to the center of our study region. It is difficult to interpret these variations without knowledge of the exact depths of tremor, but this implies that the depth of tremor changes across the Rivera–Cocos plate boundary.

When we examine the along-strike distribution of tremor source locations in time (Fig. 8), the source locations obtained for the different episodes have a complicated pattern that is difficult to generalize. As expected from the scanning for tremor

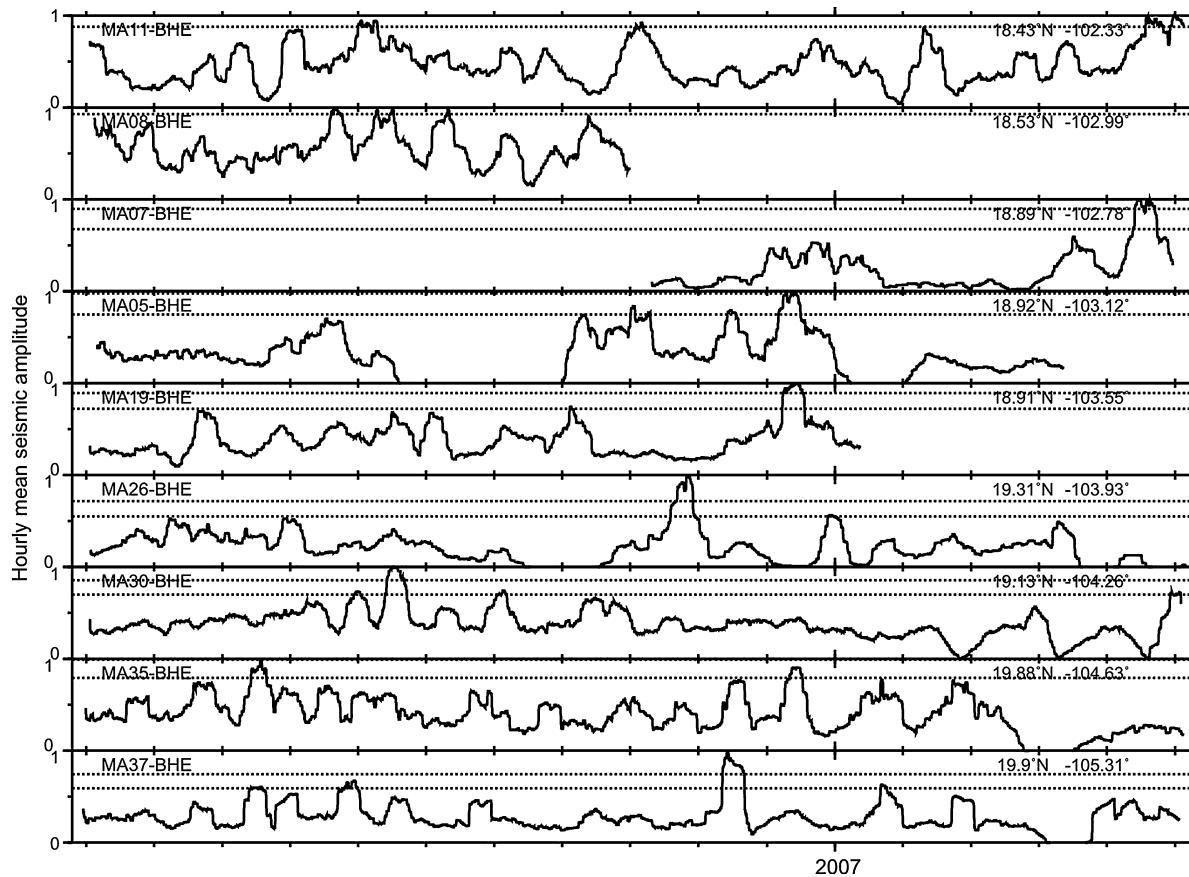


**Fig. 5.** Results of an automated scan for tremor at individual stations based on the technique of Brudzinski and Allen (2007). Smoothed time series of hourly mean amplitudes in the tremor passband are shown for the highest quality stations used in this study, ordered from east to west. Dotted lines show the  $2\sigma$  and  $3\sigma$  variation from the average value for the smoothed time series and represent time periods when seismic signals rise above background noise at greater than 95% and 99% confidence interval, respectively. Peaks are times when the tremor passband is most active and suggest tremor is prominent near those stations.

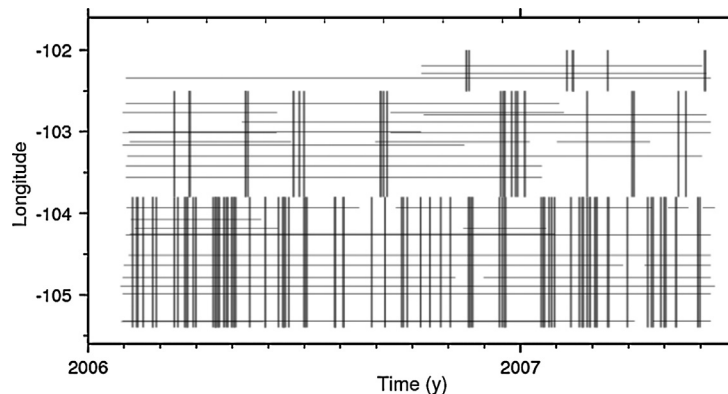


**Fig. 6.** Vertical lines are times when strong tremor has been visually identified in either the western, central, or eastern regions of the network. Horizontal lines are record times of stations suitable for detecting tremor.

signals (Fig. 6), we find many short episodes with relatively short along-strike extent (Fig. 8). Most episodes analyzed in this study last for only a few days and result in a distribution of epicenters about 50 km wide. A few episodes that last upwards of a week result in larger distributions of close to 100 km width (Fig. 8). However, none of the events reach the broad ( $>200$  km) size of the larger events in Cascadia that migrate along-strike at  $\sim 10$  km/day over several weeks. None of the episodes in our study region show evidence of clear along-strike migration.

Fig. 8 helps to illustrate that the western part of the network appears to have been more frequently active than the eastern part

of the network. In particular, we find there are periods where tremor appears to recur almost monthly west of  $105^\circ\text{W}$  and bi-monthly between  $104.5$ – $105^\circ\text{W}$ , although it is still possible that the slight differences in location from episode to episode indicate that the patch of tremor activity may not be identical each time. The latter region also has a curious case where tremor appears to be recurrent or stationary over a two week time span in December 2006. Autocorrelation analysis to search for low-frequency earthquakes and subsequent cross-correlation of similar waveforms to refine source locations may be able to further investigate these interesting features.

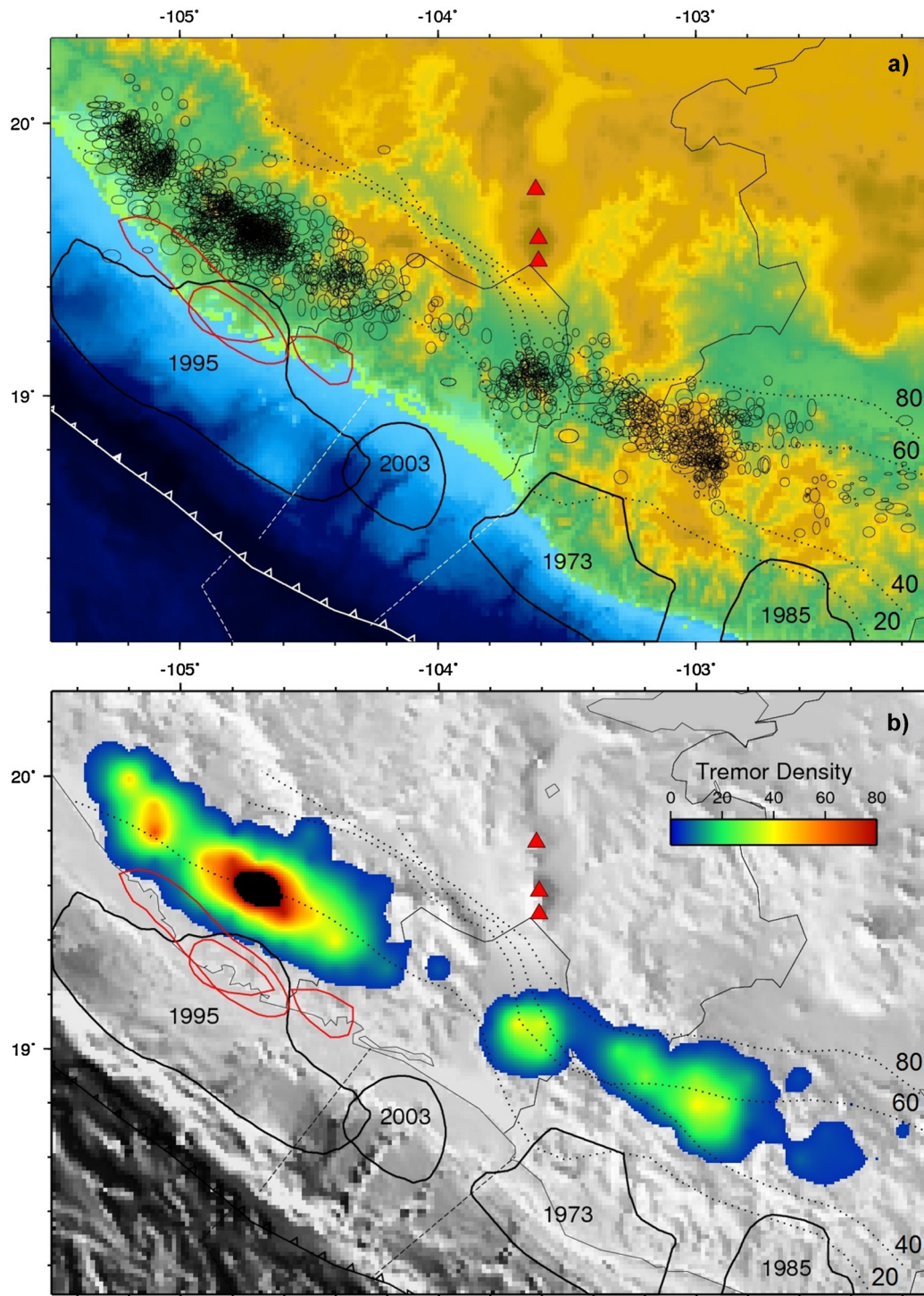


**Fig. 7.** Results of tremor identification and source location. (a) Ellipses are centered on determined epicenter and size shows horizontal uncertainties. Layout as in Fig. 2. (b) Color shading indicates density of detected tremor epicenters, which estimates the prevalence of tremor along the margin. Layout as in Fig. 2 except topography is now gray-shaded. (For interpretation of the references to color in this figure legend, the reader is referred to the web version of this article.)

The frequent recurrence of tremor episodes in this region resembles that of Oaxaca and Nankai, where short tremor episode recurrences on the order of 3–6 months have been observed (Obara et al., 2004; Brudzinski et al., 2010). Patches of even more frequently active tremor like that in western Jalisco have also been identified in Nankai (Ide et al., 2010). The similarity between Nankai and Mexico is further revealed when one also considers that the region of tremor recurrence is offset from the seismogenic zone (Fig. 7) (e.g., Brudzinski et al., 2010).

#### 4. Lack of tectonic tremor associated with subducted boundary between Rivera and Cocos

One of the most intriguing features in the distribution of tectonic tremor is the apparent gap beneath the western portion of the Colima Graben and immediately southwest of the Fuego de Colima and Nevado de Colima volcanoes (Fig. 7). Located onshore from the western half of the Manzanillo Trough, these features may represent the surface expression of the subducted bound-

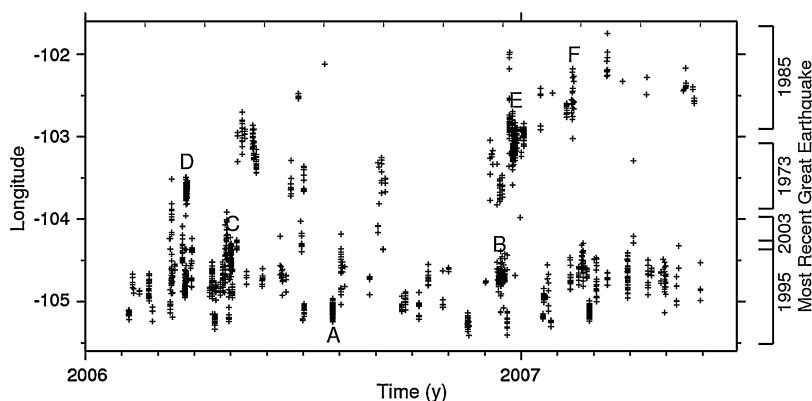


**Fig. 8.** Along-strike locations of tremor versus time. Episodes shown in Fig. 3 are labeled accordingly. Tremor episodes appear to have some regularity in the along-strike extent.

ary between the Rivera and Cocos plates (Singh et al., 1985; Bandy et al., 1995). The fact that the volcanoes are offset towards the trench relative to the Trans-Mexican Volcanic Belt has been suggested to represent evidence that the plates separate after subduction, such that material upwelling between them shifts volcanism closer to the trench than would otherwise be the case (Yang et al., 2009). This hypothesis would provide a ready explanation for the lack of tremor, as perturbation to the typical subduction interface would disrupt the physical conditions. While the lack of a coherent subducting plate to host the appropriate fault interface throughout the tremor gap is one possibility, another is that a small break between subducting plates disturbs the conditions that may be necessary to generate tremor (Fagereng and Diener, 2011; Hyndman et al., 2015).

Tremor gaps observed in Cascadia and Nankai provide a useful comparison. The two most prominent gaps in Cascadia occur on Vancouver Island and near the Oregon–California border. The former has been interpreted as due to recent large crustal earthquakes that reduce the stress in the tremor source zone (Kao et al., 2009), but there is no evidence to support that explanation in the latter region (Gomberg and Grp, 2010), nor is there evidence for recent large crustal earthquakes exclusively in the Colima tremor gap. An alternative interpretation is that the gaps align with the subducted boundaries between the Gorda, Juan de Fuca, and Explorer plates (Boyarko and Brudzinski, 2010), which is consistent with the interpretation in Colima. Further support for this notion comes from Nankai, where a prominent gap in tremor is attributed by Ide et al. (2010) to an abrupt change of subduction direction caused by a split in the subducted plate along an extinct ridge. Considering the volcanism immediately northwest of the gap in Colima and tomographic evidence that the Rivera and Cocos plates are separated by 150 km depth (Yang et al., 2009), we propose that plate separation after subduction is the most likely explanation for the tremor gap. The model presented by Yang et al. (2009) would suggest there is no physical tear in the subducting plate at the depth of tremor and a warm temperature anomaly due to tearing at greater depth and subsequent upwelling causes the gap in tremor by disturbing the conditions needed for tremor. However, it appears the tear between the subducting plates occurs at shallower depths considering the recent relocation of seismicity that shows distinctly different slab dips on either side of the gap (e.g., Abbott and Brudzinski, 2015). Moreover, recently observed elevated  $^3\text{He}/^4\text{He}$  in springs of the Colima graben and those further to the south also requires decoupling of the subducting plates near the trench (Taran et al., 2013). Our results further support the notion that the plates separate quickly after subduction, which has implications for our tectonic and seismogenic understanding of subducted plate boundaries, as we note that recent large megath-

rust earthquakes have not ruptured across this gap (Schmitt et al., 2007).

### 5. Evidence for slow slip events in the Jalisco region

Previous studies found no evidence for slow slip events (SSE) in Jalisco back to early 1993, but were hindered by a combination of the sparse station distribution prior to 2007 and the low amplitude of the SSE that appears to characterize the northwestern end of the Mexico Subduction Zone (Marquez-Azua et al., 2002; Marquez-Azua and DeMets, 2009). Six continuous GPS stations were operating in western Mexico during approximately the first year of the MARS deployment (Fig. 9). Of these, only three stations were close enough to the Pacific coast to record any SSE that may have occurred during the seismic deployment, namely, sites COLI, COOB, and UCOL. None of these sites show compelling evidence for SSE between 2006 and mid-2007 (Fig. 9), suggesting that the abundant tremor detected from the MARS seismic data is unrelated to SSE large enough to be detected with GPS. Transient motion in late 2005–early 2006 at site UCOL is strongly correlated in time with the regional common-mode noise (Fig. 9) and is unlikely to represent SSE.

Significant improvements in the GPS station density and distribution began in late 2006 during the MARS deployment. Although these occurred too late to reliably document any SSE during the seismic deployment, they provide a strong basis for examining the broader question of whether SSE occurs along the Rivera and northern Cocos subduction interfaces. In particular, 19 continuous GPS sites in the region have operated at various times since late 2006 and are considered herein (Figs. 9 and 10 and Supplemental Figs. S1–S6). We describe their position time series from 2006.0 to the present and highlight the first evidence for SSE in this region. Our procedures for processing the raw GPS observations are described in the supplement along with a description and demonstration of the method to estimate and correct for non-tectonic, spatially correlated noise between stations.

The clearest evidence for SSE in our study region was recorded by GPS stations MOGA, UCOE, and UGTO (blue in Fig. 10), all located above the subducting Cocos plate. Before 2014.0, slow inland motion was recorded at these sites, representing inter-seismic shortening from NE-directed Cocos–North America plate convergence. At 2014.0, transient eastward motions began at all three stations, coinciding with the well-described Guerrero SSE (Radiguet, 2016). At site MMIG near the coast, a subtle velocity change at 2014.0 and resumption of rapid northeastward motion in late 2014 (Fig. 10) also coincide with the beginning and end of the 2014 Guerrero SSE.

Evidence for an SSE in mid-2011 is also seen at coastal site MMIG above the subducting Cocos plate (Figs. 10, S6, and S7). The



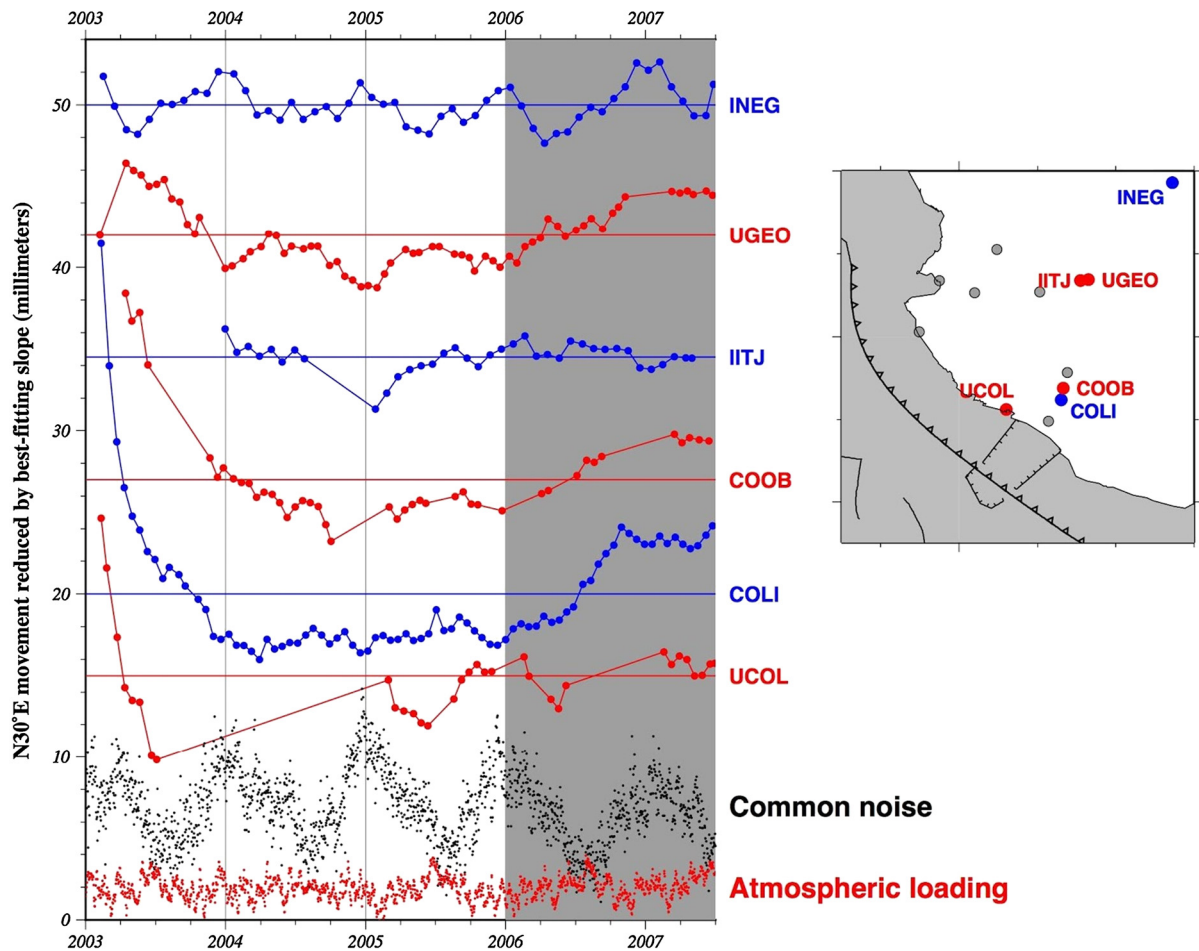


**Fig. 9.** Position time series for GPS stations in western Mexico that were operating from 2003 to 2007.5, including the MARS seismic deployment indicated by the gray-shaded region. The red and blue circles show 20-day average positions estimated from daily site locations, corrected for daily common-mode noise (black circles), and rotated onto N30°E, the plate convergence direction. Each GPS position time series is reduced by its best-fitting slope for the period 2003.0 to 2007.5. Daily displacements predicted for atmospheric pressure loading ([ggosatm.hg.tuwien.ac.at](http://ggosatm.hg.tuwien.ac.at)) are shown for comparison at the bottom of the figure. (For interpretation of the references to color in this figure legend, the reader is referred to the web version of this article.)

amplitude of this previously undescribed SSE is roughly twice the amplitude of the regional, non-tectonic noise (Fig. S6) and is thus unlikely to be an artifact of the method we use to correct for that noise. TECO, the site closest to MMIG, exhibits a simultaneous, smaller amplitude change in station motion (Figs. 10 and S7), as do COLI, COOB, and possibly NVDO in the southern Colima Rift (Fig. S5). This SSE appears to originate on the Cocos plate interface near the southern Colima graben. Unfortunately, data gaps at MMIG and TECO preclude a precise determination of the duration and amplitude of this likely SSE.

Identifying SSE that originates on the Rivera plate interface is more challenging. In contrast to SSE elsewhere in southern Mexico (Figs. S9 and S10), any 2006–2016 deformation attributable to SSE on the Rivera subduction interface was small and close to the underlying noise in the GPS position time series. Clear evidence for SSE is best seen in 2008 and 2013 for station CHMC along the Jalisco coast (Figs. 10, S2, and S7). The first SSE had an amplitude roughly twice that of the seasonal noise (Fig. S2) and  $\sim 5$  times that of the modeled atmospheric loading (Fig. 10). Subtle, similarly timed changes in motion were recorded at stations PURI and PZUL directly inland and northwest of site CHMC (Fig. S2 and 10). The absence of any corresponding change in motion at sites UCOM and TECO in 2008 strongly suggests that the SSE originated northwest of the southern Colima Rift. This is the first evidence for SSE originating on the Rivera plate subduction interface. Corroborating evidence for the 2013 SSE seen at CHMC is limited to sites PENA and

possibly UCOM, MASC, and MPR1 (Figs. 10 and S8), where low-amplitude, simultaneous changes in motion were recorded. Other GPS stations in the vicinity of these sites (PURI, TECO, PZUL, COOB) were not recording in late 2013.

Several stations closer to the trench (PENA, TECO, UCOM, and COLI) have corrected, residual time series that are clearly out of phase with the regional seasonal noise (Figs. 10, S4, and S5). The annual variations at PENA are a factor-of-two larger than those attributable to atmospheric loading (Fig. S9), but are nearly the same amplitude as the regional noise (Fig. S4). Whether these signals are caused by small, annual subduction-related slow slip or instead indirectly record a weather-related phenomenon that is out of phase at locations closer to the Pacific coast than at locations farther inland is unknown. Although the nearly perfect regularity in the annual peaks at site PENA argues against a tectonic origin for the periodic signal at this site, periodic tremor and SSE have been observed in other regions (e.g., Rogers and Dragert, 2003) and nearly-annual signals have been predicted for Mexico (Lowry, 2006). Distinguishing tectonic from non-tectonic causes for these variations will be a challenge given that the amplitude of any slow slip is comparable to the amplitude of the common-mode noise. In any case, the SSE being recorded in Jalisco are an order-of-magnitude than in Guerrero and Oaxaca (Figs. S9 and S10) (Kostoglodov et al., 2003; Brudzinski et al., 2007; Radiguet et al., 2012; Graham et al., 2015).

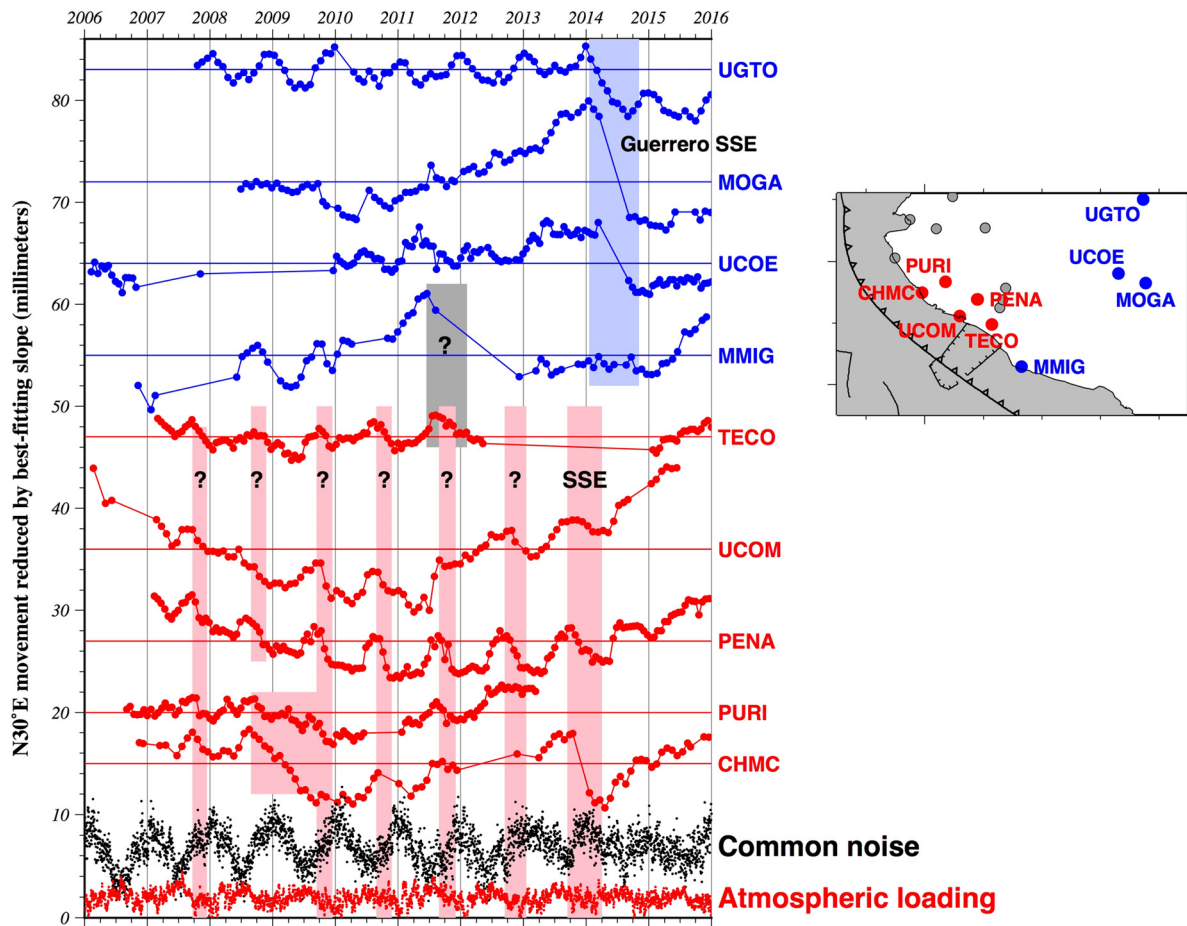


**Fig. 10.** Position time series, 20-day-averages, of selected GPS sites above the subducting Rivera (red) and Cocos (blue) plates. North and east components are rotated onto N30°E, the direction of plate convergence, and reduced by the best-fitting slope for the period 2006–2016. All position time series are corrected for the common-mode noise depicted near the bottom of the figure, but not for the calculated atmospheric loading at the bottom of the figure. The shaded vertical bars indicate periods of possible silent slip, as discussed in the text. (For interpretation of the references to color in this figure legend, the reader is referred to the web version of this article.)

## 6. Comparisons of tremor and slow slip to previous Megathrust earthquakes and Afterslip

Considering the varying along-strike history of megathrust earthquakes, we can compare the distribution of tremor with the spatial and temporal characteristics of previous great earthquakes. We focus initially on the time since the previous megathrust earthquake as this indicates to some degree the current point each region is in the earthquake cycle. Some modeling studies have suggested that recurrence intervals of episodic tremor and slip would change systematically over the course of the earthquake cycle (e.g., Liu and Rice, 2007; Matsuzawa et al., 2010). Inland from the most recent 2003 earthquake we find a prominent gap in tremor and a cluster of active tremor with a moderate recurrence interval. Inland from the 1995 earthquake we find two clusters of tremor with relatively frequent tremor. Immediately west of this region is another cluster of tremor with the most frequent tremor, but this appears to be inland from a region that has not had megathrust rupture since 1932. Inland from the 1973 is a small gap in tremor and a cluster of tremor with moderate recurrence. There is tremor inland from the 1985 earthquake that appears to be similar in nature to that inland from the 1973 event, but less instrumentation in this region makes the characterizations uncertain. While our observations of tremor are limited to a relatively short (18 month) part of the earthquake cycle and there may be other geologic factors that cause variable expressions of tremor along-strike (Brudzinski and Allen, 2007), it does not appear that progression through the earthquake cycle has a dominant role in determining the character-

istics of tremor. It may therefore be difficult to generalize tremor prevalence and recurrence as a means to forecasting the next anticipated megathrust earthquake. As an alternative, other modeling efforts have suggested that recurrence interval of tremor would increase with increasing width of the tremor region (Liu and Rice, 2009). However, we find no evidence of a correlation in our study region as the region with the widest tremor zone has one of the shortest recurrence intervals (Figs. 7 and 8).

We next examine the spatial offset of the prominent tremor band relative to the megathrust earthquake rupture zones. This feature has been examined and discussed in several recent studies (e.g., Hyndman et al., 2015; Wang and Tréhu, 2016). In our study region, this offset ranges from 5 to 40 km, assuming the rupture models accurately measure the spatial extent of megathrust slip. The average offset in this region is considerably smaller than that in Oaxaca (~50 km) and Guerrero (~80 km) (Fig. 1). This variation may be related to the expressions of episodic slow slip, as the region with the largest offset, Guerrero, has the largest slow slip episodes (Radiguet et al., 2012), while the region with the shortest offset, our study region, has much smaller GPS-detectable slow slip episodes. One possible explanation for the variation in offsets and magnitude of slow slip is the influence of slab dip. Shallow slab dip in southern Mexico (Fig. 1) places large areas of the plate interface in the appropriate conditions for transient slip (e.g., temperature, pressure, mineralogy). The steeper dip of the Rivera and western Cocos plate interface could mean that the plate interface spends less time in the appropriate conditions for tremor and slow slip. As a consequence, relatively narrow bands of the interface

may be at the right conditions for any given frictional behavior, leading to closer spacing, narrower slip zones, and smaller surface displacements. In a similar way, if our study region has a shallower continental Moho depth, it could contribute to a smaller gap between the seismogenic zone and the tremor band (Hyndman et al., 2015).

Another factor that could influence the size of GPS-detectable slow slip is the amount of afterslip that occurs following megathrust earthquakes. Observations before and after the Mw 7.6 September 2012 Nicoya, Costa Rica earthquake indicate the slip regions for slow slip and afterslip have very little overlap (Malservigi et al., 2015). This suggests that frictional properties on their respective plate interface regions are substantially different. To see whether this influences slow slip in our study region, we turn our attention to the previous analysis of afterslip following the 1995 and 2003 earthquakes offshore Jalisco and Colima. Within one week of the 1995 earthquake, post-seismic slip migrated downdip to depths of 16–35 km (Figs. 1–2, 7), where it has since decayed logarithmically (Hutton et al., 2001; Marquez-Azua et al., 2002). The relative lack of afterslip in shallow regions of the subduction interface suggests that the interface lies in the unstable frictional regime and hence is strongly coupled between earthquakes. By 1999, the cumulative slip moment associated with post-seismic slip equaled 70% of the coseismic moment, with nearly all of this slip occurring downdip from the coseismic rupture zone. A comparison of the cumulative post-seismic slip for the 2003 earthquake that can be inferred separately from earthquake aftershocks and GPS measurements within a year of the earthquake indicates that 95% or more of the post-seismic deformation was aseismic (Schmitt et al., 2007). Near-term post-seismic measurements indicate that slip propagated downdip to areas of the subduction interface beneath the coastline within days following the earthquake, similar to that of the 1995 earthquake. As such, we suggest the lack of large GPS-detected slow slip episodes in our study region is due in part to the prevalent afterslip between the seismogenic zone and the band of tremor, further restricting the portion of the plate interface that can produce episodic slow slip. Improved geodetic recording in our study region to better constrain the source region of slow slip would help to test this idea.

An intermingling of slow slip (so called “long-term” events that can last several years) and afterslip also appears to fill the gap between megathrust earthquakes and tremor in Nankai (Wang and Tréhu, 2016). In this case, we are using the discrepancy between seismic and geodetic estimates of the 1944 and 1946 earthquakes to approximate the location of afterslip. The situation in Cascadia is less clear because there is no evidence that slow slip occurs in the gap (e.g., Holtkamp and Brudzinski, 2010; Hyndman et al., 2015), and there are no estimates of afterslip following the 1700 earthquake. Holtkamp and Brudzinski (2010) have suggested this could be a permanent gap between the seismogenic zone and slow slip zone based on low levels (<40%) of plate interface locking. Although the low levels of coupling could still result in afterslip following a megathrust earthquake, afterslip following the 2012 Costa Rica earthquake was focused in an area with interseismic locking >50%.

The migration of slip after 1995 megathrust earthquake to a deeper and presumably velocity-strengthening area of the subduction interface and the logarithmic decay of afterslip conform to the qualitative and quantitative predictions of a model in which the fault kinematics are prescribed by rate- and state-variable frictional laws (Scholz, 2002). While this conforms to the traditional view of a fairly abrupt frictional stability transition from velocity-weakening to velocity-strengthening, it is somewhat in contrast to the Guerrero and Oaxaca regions where the episodic slow slip is directly adjacent to the previous megathrust rupture zones (Fig. 1). These areas appear to be similar to areas of Nankai, where episodic

release of accumulated strain in the form of long-term slow slip seems to indicate a velocity weakening behavior in order to initiate slip acceleration but that the slip is somehow regulated (e.g., dilatancy stabilization) to prevent it from reaching seismogenic speeds (Segall et al., 2010). Finally, both the regions of afterslip and the regions of episodic slow slip are then juxtaposed by a deeper region of frequently recurring tremor episodes, which seems to indicate yet another mode of the frictional stability transition or that tremor requires a slightly different set of physical conditions. Higher resolution observations from Nankai suggest that these prevalent tremor episodes are driven by shorter duration (“short-term”) slow slip episodes on the deeper parts of the subduction interface with transient slip detectable on tiltmeters that are difficult to observe via GPS (e.g., Obara et al., 2004). Unfortunately, such high resolution geodetic instruments do not currently exist in this region, but we hypothesize that tremor episodes in this region are also coincident with smaller amounts of short-term slow slip.

## 7. Conclusions

This study presents several pieces of evidence for tectonic tremor beneath the states of Jalisco, Colima and Michoacán, Mexico. This tremor is particularly frequent in the western end of the study region, and resembles that of so-called “short-term” events seen in Nankai where the geodetic signature is small enough to be buried in the uncertainty of typical GPS time series. The spatial extent of individual events is also relatively small, and there is no evidence during the 18 months of recording for broad (>200 km) along-strike migrating events like that seen in Cascadia. However, the along-strike distribution of tremor still outlines areas of more frequent tremor occurrence, as well as a prominent tremor gap beneath the western portion of the Colima Graben. Considering that tremor gaps have also been interpreted as due to gaps in the subducting plate in Nankai and Cascadia, we propose that the tremor gap marks the shallow separation between the subducting Cocos and Rivera plates that facilitates upwelling and volcanism further inland.

Comparison to previous megathrust earthquakes in the region revealed no apparent patterns between the time elapsed since the last great earthquake and the spatial or temporal distribution of tremor. Tremor episodes recurred most frequently in the region ~10 yr into the interseismic cycle, least frequently in the region 3–4 yr into the interseismic cycle, and moderately frequently in the region ~30 yr into the interseismic cycle. While there are likely several influences on the tremor episode recurrence and our data only sampled a small portion of the interseismic cycle, this result does not provide evidence that one can use the tremor recurrence alone to interpret when the next great earthquake is due.

Daily positions recorded between 2006 and 2016 at 19 continuous GPS stations in western Mexico clearly reveal slow slip events presumably originating on the northern Cocos plate and Rivera plate subduction interfaces. Stations located above the subducting Cocos plate record the previously described 2014 Guerrero SSE, and may record a previously unrecognized SSE in 2011. We also describe the first evidence for SSE (in 2008 and 2013) on the Rivera plate subduction interface, albeit with much smaller amplitude and more localized effects than SSE that originates on the nearly-flat subduction interface below southern Mexico. Additional, annual variations in the positions of a subset of GPS stations directly above the Rivera plate interface may also be recording regular SSE given that the variations are out of phase with the regional GPS station position noise and have amplitudes that are too large to be explained via atmospheric pressure loading.

The spatial separation between the megathrust earthquakes and tremor band did not show coherent variations across our study region, but the separation was generally smaller than that observed

previously in Guerrero and Oaxaca, Mexico, which may indicate it is a function of slab dip. One potentially related difference is that prominent afterslip following the 1995 and 2003 earthquakes may further restrict the area of plate interface available for slow slip episodes.

### Acknowledgements

Support for this work was provided by NSF Grants EAR-0847688 (MB), EAR-0510553 (CD) and EAR-1114174 (CD). We are grateful to the entire MARS team for collecting an important seismic dataset, and thank IRIS PASSCAL for their support of the deployment and the IRIS DMC for serving the data. We also utilized GPS data archived at the UNAVCO Facility with support from the National Science Foundation (NSF) and National Aeronautics and Space Administration under NSF Cooperative Agreement No. EAR-0735156. This material is based partly on data provided by the Trans-boundary, Land and Atmosphere Long-term Observational and Collaborative Network (TLALOCnet) operated by UNAVCO and supported by the National Science Foundation No. EAR-1338091. S. Fasola helped improve this manuscript.

### Appendix A. Supplementary material

Supplementary material related to this article can be found online at <http://dx.doi.org/10.1016/j.epsl.2016.08.004>.

### References

- Abbott, E.R., Brudzinski, M.R., 2015. Shallow seismicity patterns in the northwestern section of the Mexico Subduction Zone. *J. South Am. Earth Sci.* 63, 279–292. <http://dx.doi.org/10.1016/j.jsames.2015.07.012>.
- Bandy, W., Mortera-Gutiérrez, C., Urrutia-Fucugauchi, J., Hilde, T.W.C., 1995. The Subducted Rivera-Cocos plate boundary – where is it, what is it, and what is its relationship to the colima rift. *Geophys. Res. Lett.* 22, 3075–3078. <http://dx.doi.org/10.1029/95GL03055>.
- Bandy, W.L., Kostoglodov, V.V., Mortera-Gutiérrez, C.A., Urrutia-Fucugauchi, J., 1998. Comment on “Relative motions of the Pacific, Rivera, North American, and Cocos plates since 0.78 Ma” by Charles DeMets and Douglas S. Wilson. *J. Geophys. Res., Solid Earth* 103, 24245–24250.
- Boyarko, D.C., Brudzinski, M.R., 2010. Spatial and temporal patterns of nonvolcanic tremor along the southern Cascadia subduction zone. *J. Geophys. Res., Solid Earth* 115, B00A22. <http://dx.doi.org/10.1029/2008JB006064>.
- Brown, J.R., Beroza, G.C., Ide, S., Ohta, K., Shelly, D.R., Schwartz, S.Y., Rabbel, W., Thorwart, M., Kao, H., 2009. Deep low-frequency earthquakes in tremor localize to the plate interface in multiple subduction zones. *Geophys. Res. Lett.* 36, L19306. <http://dx.doi.org/10.1029/2009GL040027>.
- Brudzinski, M., Cabral-Cano, E., Correa-Mora, F., DeMets, C., Márquez-Azúa, B., 2007. Slow slip transients along the Oaxaca subduction segment from 1993 to 2007. *Geophys. J. Int.* 171, 523–538. <http://dx.doi.org/10.1111/j.1365-246X.2007.03542.x>.
- Brudzinski, M.R., Allen, R.M., 2007. Segmentation in episodic tremor and slip all along Cascadia. *Geology* 35, 907–910. <http://dx.doi.org/10.1130/G23740A.1>.
- Brudzinski, M.R., Hinojosa-Prieto, H.R., Schlanser, K.M., Cabral-Cano, E., Arciniega-Ceballos, A., Diaz-Molina, O., DeMets, C., 2010. Nonvolcanic tremor along the Oaxaca segment of the Middle America subduction zone. *J. Geophys. Res., Solid Earth* 115, B00A23. <http://dx.doi.org/10.1029/2008JB006061>.
- Cruz-Jiménez, H., Chávez-García, F.J., Furumura, T., 2009. Differences in attenuation of ground motion perpendicular to the Mexican subduction zone between Colima and Guerrero: an explanation based on numerical modeling. *Bull. Seismol. Soc. Am.* 99, 400–406. <http://dx.doi.org/10.1785/0120080167>.
- Currie, C.A., Hyndman, R.D., Wang, K., Kostoglodov, V., 2002. Thermal models of the Mexico subduction zone: implications for the megathrust seismogenic zone. *J. Geophys. Res., Solid Earth* 107, 2370. <http://dx.doi.org/10.1029/2001JB000886>.
- DeMets, C., Wilson, D.S., 1997. Relative motions of the Pacific, Rivera, North American, and Cocos plates since 0.78 Ma. *J. Geophys. Res., Solid Earth* 102, 2789–2806. <http://dx.doi.org/10.1029/96JB03170>.
- Fagereng, Á., Diener, J.F.A., 2011. Non-volcanic tremor and discontinuous slab dehydration. *Geophys. Res. Lett.* 38, L15302. <http://dx.doi.org/10.1029/2011GL048214>.
- Fasola, S., Brudzinski, M.R., Ghouse, N., Solada, K., Sit, S.M., Cabral-Cano, E., Arciniega-Ceballos, E.A., Kelly, N., Jensen, K., 2016. New perspective on the transition from flat to steeper subduction in Oaxaca, Mexico, based on seismicity, nonvolcanic tremor, and slow slip. *J. Geophys. Res., Solid Earth* 121. <http://dx.doi.org/10.1002/2015JB012709>.
- Frank, W.B., Radiguet, M., Rousset, B., Shapiro, N.M., Husker, A.L., Kostoglodov, V., Campillo, M., 2015. Uncovering the geodetic signature of silent slip through repeating earthquakes. *Geophys. Res. Lett.* 42, 2774–2779. <http://dx.doi.org/10.1002/2015GL063685>.
- Gomberg, J., Grp, C.W., 2010. Slow-slip phenomena in Cascadia from 2007 and beyond: a review. *Geol. Soc. Am. Bull.* 122, 963–978. <http://dx.doi.org/10.1130/B30287.1>.
- Graham, S., DeMets, C., Cabral-Cano, E., Kostoglodov, V., Rousset, B., Walpersdorf, A., Cotte, N., Lasserre, C., McCaffrey, R., Salazar-Tlaczani, L., 2015. Slow slip history for the Mexico subduction zone: 2005 through 2011. *Pure Appl. Geophys.*, 1–21. <http://dx.doi.org/10.1007/s00024-015-1211-x>.
- Hermann, R.-B., 2004. Computer programs in seismology. Version 3.30-GSAC.
- Holtkamp, S., Brudzinski, M.R., 2010. Determination of slow slip episodes and strain accumulation along the Cascadia margin. *J. Geophys. Res., Solid Earth* 115. <http://dx.doi.org/10.1029/2008JB006058>.
- Hutton, W., DeMets, C., Sanchez, O., Suárez, G., Stock, J., 2001. Slip kinematics and dynamics during and after the 1995 October 9 Mw=8.0 Colima-Jalisco earthquake, Mexico, from GPS geodetic constraints. *Geophys. J. Int.* 146, 637–658. <http://dx.doi.org/10.1046/j.1365-246X.2001.00472.x>.
- Hyndman, R.D., McCrory, P.A., Wech, A., Kao, H., Ague, J., 2015. Cascadia subducting plate fluids channelled to fore-arc mantle corner: ETS and silica deposition. *J. Geophys. Res., Solid Earth* 120, 4344–4358.
- Ide, S., Shiomi, K., Mochizuki, K., Tonegawa, T., Kimura, G., 2010. Split Philippine sea plate beneath Japan. *Geophys. Res. Lett.* 37 (21), 1–6. <http://dx.doi.org/10.1029/2010GL044585>.
- Ito, Y., Obara, K., Shiomi, K., Sekine, S., Hirose, H., 2007. Slow earthquakes coincident with episodic tremors and slow slip events. *Science* 315, 503–506. <http://dx.doi.org/10.1126/science.1134454>.
- Jödicke, H., Jording, A., Ferrari, L., Arzate, J., Mezger, K., Rupke, L., 2006. Fluid release from the subducted Cocos plate and partial melting of the crust deduced from magnetotelluric studies in southern Mexico: implications for the generation of volcanism and subduction dynamics. *J. Geophys. Res., Solid Earth* 111, B08102. <http://dx.doi.org/10.1029/2005JB003739>.
- Kao, H., Shan, S.-J., Dragert, H., Rogers, G., 2009. Northern Cascadia episodic tremor and slip: a decade of tremor observations from 1997 to 2007. *J. Geophys. Res.* 114, B00A12. <http://dx.doi.org/10.1029/2008JB006046>.
- Kostoglodov, V., Singh, S.K., Santiago, J.A., Franco, S.L., Larson, K.M., Lowry, A.R., Bilham, R., 2003. A large silent earthquake in the Guerrero seismic gap, Mexico. *Geophys. Res. Lett.* 30, 1807. <http://dx.doi.org/10.1029/2003GL017219>.
- Liu, Y., Rice, J.R., 2007. Spontaneous and triggered aseismic deformation transients in a subduction fault model. *J. Geophys. Res., Solid Earth* 112, B09404. <http://dx.doi.org/10.1029/2007JB004930>.
- Liu, Y., Rice, J.R., 2009. Slow slip predictions based on granite and gabbro friction data compared to GPS measurements in northern Cascadia. *J. Geophys. Res., Solid Earth* 114, B09407. <http://dx.doi.org/10.1029/2008JB006142>.
- Lowry, A.R., 2006. Resonant slow fault slip in subduction zones forced by climatic load stress. *Nature* 442 (7104), 802–805. <http://dx.doi.org/10.1038/nature05055>.
- Malservisi, R., Schwartz, S.Y., Voss, N., Protti, M., Gonzalez, V., Dixon, T., Jiang, Y., Newman, A.V., Richardson, J., Walter, J.L., Vayenko, D., 2015. Multiscale post-seismic behavior on a megathrust: the 2012 Nicoya earthquake, Costa Rica. *Geochim. Geophys. Geosyst.* 16. <http://dx.doi.org/10.1002/2015GC005794>.
- Marquez-Azua, B., DeMets, C., 2009. Deformation of Mexico from continuous GPS from 1993 to 2008. *Geochim. Geophys. Geosyst.* 10, Q02003. <http://dx.doi.org/10.1029/2008GC002278>.
- Marquez-Azua, B., DeMets, C., Masterlark, T., 2002. Strong interseismic coupling, fault afterslip, and viscoelastic flow before and after the Oct. 9, 1995 Colima-Jalisco earthquake: continuous GPS measurements from Colima, Mexico. *Geophys. Res. Lett.* 29, 1281. <http://dx.doi.org/10.1029/2002GL014702>.
- Matsuzawa, T., Hirose, H., Shibasaki, B., Obara, K., 2010. Modeling short- and long-term slow slip events in the seismic cycles of large subduction earthquakes. *J. Geophys. Res., Solid Earth* 115 (B12). <http://dx.doi.org/10.1029/2010JB007566>.
- Mendoza, C., 1993. Coseismic slip of 2 large Mexican earthquakes from teleseismic body wave-forms: implications for asperity interaction in the Michoacan plate boundary segment. *J. Geophys. Res., Solid Earth* 98, 8197–8210. <http://dx.doi.org/10.1029/93JB00021>.
- Mendoza, C., Hartzell, S., 1999. Fault-slip distribution of the 1995 Colima-Jalisco, Mexico, earthquake. *Bull. Seismol. Soc. Am.* 89, 1338–1344.
- Obara, K., 2002. Nonvolcanic deep tremor associated with subduction in southwest Japan. *Science (N.Y.)* 296, 1679–1681. <http://dx.doi.org/10.1126/science.1070378>.
- Obara, K., Hirose, H., Yamamizu, F., Kasahara, K., 2004. Episodic slow slip events accompanied by non-volcanic tremors in southwest Japan subduction zone. *Geophys. Res. Lett.* 31, L23602. <http://dx.doi.org/10.1029/2004GL020848>.
- Pardo, M., Suárez, G., 1995. Shape of the subducted Rivera and Cocos plates in southern Mexico: seismic and tectonic implications. *J. Geophys. Res., Solid Earth* 100, 12357–12373.
- Payero, J.S., Kostoglodov, V., Shapiro, N., Mikumo, T., Iglesias, A., Perez-Campos, X., Clayton, R.W., 2008. Nonvolcanic tremor observed in the Mexican subduction zone. *Geophys. Res. Lett.* 35, L07305. <http://dx.doi.org/10.1029/2007GL032877>.
- Radiguet, M., 2016. The large 2014 slow slip event in Guerrero, Mexico: new feature and possible triggering of the 18 April Papanoa earthquake (Mw 7.3). In: AGU Chapman Conference on the Slow Slip Phenomena. Ixtapa, MX, Feb. 23, 2016.

- Radiguet, M., Cotton, F., Vergnolle, M., Campillo, M., Walpersdorf, A., Cotte, N., Kostoglodov, V., 2012. Slow slip events and strain accumulation in the Guerrero gap, Mexico. *J. Geophys. Res., Solid Earth* 117, B04305. <http://dx.doi.org/10.1029/2011JB008801>.
- Reyes, A., Brune, J.N., Lomnitz, C., 1979. Source mechanism and aftershock study of the Colima, Mexico earthquake of January 30, 1973. *Bull. Seismol. Soc. Am.* 69, 1819–1840.
- Rogers, G., Dragert, H., 2003. Episodic tremor and slip on the Cascadia subduction zone: the chatter of silent slip, vol. 300. *Science, New York, N.Y.*, pp. 1942–1943.
- Schmitt, S.V., DeMets, C., Stock, J., Sanchez, O., Marquez-Azua, B., Reyes, G., 2007. A geodetic study of the 2003 January 22 Tecoman, Colima, Mexico earthquake. *Geophys. J. Int.* 169, 389–406. <http://dx.doi.org/10.1111/j.1365-246X.2006.03322.x>.
- Scholz, C.H., 2002. *The Mechanics of Earthquakes and Faulting*. Cambridge University Press.
- Schwartz, S.Y., Rokosky, J.M., 2007. Slow slip events and seismic tremor at circum-Pacific subduction zones. *Rev. Geophys.* 45, RG3004. <http://dx.doi.org/10.1029/2006RG000208>.
- Segall, P., Rubin, A.M., Bradley, A.M., Rice, J.R., 2010. Dilatant strengthening as a mechanism for slow slip events. *J. Geophys. Res., Solid Earth* 115, B12305. <http://dx.doi.org/10.1029/2010JB007449>.
- Shelly, D.R., Beroza, G.C., Ide, S., 2007. Non-volcanic tremor and low-frequency earthquake swarms. *Nature* 446, 305–307. <http://dx.doi.org/10.1038/nature05666>.
- Singh, S.K., Ponce, L., Nishenko, S.P., 1985. The Great Jalisco, Mexico, earthquakes of 1932–subduction of the Rivera Plate. *Bull. Seismol. Soc. Am.* 75, 1301–1313.
- Song, T.-R.A., Helmlinger, D., Brudzinski, M.R., Clayton, R.W., Davis, P., Pérez-Campos, X., Singh, S.K., 2009. Subducting slab ultra-slow velocity layer coincident with silent earthquakes in southern Mexico. *Science* 324, 502–506. <http://dx.doi.org/10.1126/science.1167595>.
- Taran, Y., Morán-Zenteno, D., Inguaggiato, S., Varley, N., Luna-González, L., 2013. Geochemistry of thermal springs and geodynamics of the convergent Mexican Pacific margin. *Chem. Geol.* 339, 251–262. <http://dx.doi.org/10.1016/j.chemgeo.2012.08.025>.
- Wang, K., Tréhu, A.M., 2016. Invited review paper: some outstanding issues in the study of great megathrust earthquakes – the Cascadia example. *J. Geodyn.* 98, 1–18.
- Wech, A.G., Creager, K.C., 2008. Automated detection and location of Cascadia tremor. *Geophys. Res. Lett.* 35, L20302. <http://dx.doi.org/10.1029/2008GL035458>.
- Yang, T., Grand, S.P., Wilson, D., Guzman-Speziale, M., Gomez-Gonzalez, J.M., Dominguez-Reyes, T., Ni, J., 2009. Seismic structure beneath the Rivera subduction zone from finite-frequency seismic tomography. *J. Geophys. Res.* 114, B01302. <http://dx.doi.org/10.1029/2008JB005830>.